MgB_2 cylindrical superconducting shielding for cryogenic measurement applications: a case study on DC current transformers

2014 JINST 9 P04020

(http://iopscience.iop.org/1748-0221/9/04/P04020)

PUBLISHED BY IOP PUBLISHING FOR SISSA MEDIALAB

RECEIVED: *January 24, 2014*
ACCEPTED: *March 11, 2014*
PUBLISHED: *April 23, 2014*

MgB_2 cylindrical superconducting shielding for cryogenic measurement applications: a case study on DC current transformers

P. Arpaia,[a,b,1] **A. Ballarino,**[b] **G. Giunchi**[c] **and G. Montenero**[b]

[a] *Università del Sannio, Dipartimento di Ingegneria, Corso Garibaldi 107, 82100, Benevento, Italy*
[b] *CERN — European Laboratory for Nuclear Research, Department of Technologies, Group of Magnets, Superconductors and Cryostats, CH-1211 Geneva 23, Switzerland*
[c] *Materials Science Consultant, via Teodosio 8 Milano, Italy*

E-mail: pasquale.arpaia@cern.ch

ABSTRACT: A method for designing cylindrical hollow superconducting shields for cryogenic measurement devices operating in background fields of 1 T is proposed. The shield design is based on MgB_2 composite, manufactured by the reactive Mg liquid infiltration process [1]. The MgB_2 composite allows low-cost shields with good mechanical resistance to be realized easily. The geometrical design is benchmarked by the experimental characterization at 4.2 K. A design case study for the shield of a cryogenic DC current transformer is reported. Design results show a shielding efficiency of 70% for both the axial and radial components, with prospective measurement accuracy up to 10 ppm on 100 kA.

KEYWORDS: Instrumentation for particle accelerators and storage rings - high energy (linear accelerators, synchrotrons); Accelerator Subsystems and Technologies; Special cables; Accelerator Applications

[1] Corresponding author.

doi:10.1088/1748-0221/9/04/P04020

Contents

2014 JINST 9 P04020

1 Introduction

Nowadays, at liquid Helium temperature, Type-II superconducting alloys exhibit critical current density of the order of hundreds of $kAcm^{-2}$ in a magnetic field of several T. This is a key factor for shielding DC magnetic fields effectively. However, for the shielding efficiency, the geometry plays a crucial role.

Shielding properties of Type-II superconductors can be exploited in a variety of ways: field shaping [2, 3], field concentration [4], measurement devices [5, 6], and interfering field suppression [7]. For the last category, the superconductor can work according to the field level either in the Meissner or in the mixed state [8]. In high-field environment, superconducting shield plays a crucial role to improve sensor performance [10].

In ref. [10], the design of a cryogenic sensing element for DC current measurements up to 100 kA (e.g. DC current transformers, DCCTs [11]) is proposed. This device is conceived to operate at 4.2 K for a maximum background field of 1 T. Disturbance fields as higher than hundreds of mT affect the accuracy of the DCCT significantly. The stringent requirements of 1 T can be addressed with a multilayer ferromagnetic shield [12]. However, this constrains the device bandwidth, because the multilayer has a bigger size affecting the equivalent inductance [10]. In the DCCT design [10], a cylindrical superconducting magnetic shield (owing to the favourable temperature of operation), combined with a pure iron thin shell (2 mm thick), is exploited. From this

point of view, the shielding efficiency results from the iron's action (up to 0.3 T), combined with the hollow superconducting cylinder for the full range from 0 to 1 T. Thus, the superconducting cylinder has to guarantee an attenuation of 70% for external fields of 1 T. Further benefits from this development could be exploited in the design of other cryogenic current meters, such as in ref. [13], where the desired field attenuation is achieved in two steps, namely by a shell of PbBi for field up to 0.5 T, and a coil of NbTi, soldered on the top of the shell, up to 1.5 T.

Among the available superconducting materials, the choice of a NbTi-based composite represents a well-established solution for shielding applications. As an example, the performance of the NbTi/Nb/Cu multilayer sheet [14, 15] seems to lead to an easy realization of the cylindrical geometry needed for a cryogenic DCCT. In ref. [15], the shielding efficiency of a cylinder manufactured by deep drawing a 1-mm thick sheet is shown to reach almost 100% for fields below 1 T in parallel configuration. Moreover, the material is a multilayer composite, thus overlapping or wrapping a thinner sheet does not affect performance [15, 16].

However, drawbacks arise from the shield realization. For a typical configuration of 140 mm of inner diameter for the cylindrical annulus to be produced [10], with maximum available sheet dimensions of 130 mm $\times$ 2000 mm $\times$ 0.2 mm, at least 5 sheets have to be overlapped. Prohibitive problems arise from (i) wrapping the sheets around the DCCT, (ii) keeping tightened the assembly, and (iii) avoiding discontinuities among the layers. Therefore, beyond the shielding efficiency, new requirements for the superconducting material are imposed. Customization of the manufacturing process to produce the required object geometry is the main requirement, and mechanical stability of large parts complements the specification. Indeed, the NbTi/Ni/Cu composite has a complex fabrication process, where costs impact on the product, and customization is not available.

In ref. [17], the effectiveness of MgB_2 cylinders as passive magnetic shield at 4.2 K was proved. The applied field, parallel to the cylinder axis, was raised up to 2 T, without detecting signal outside the resolution of 10 μT of the Hall probe. During the field ramp down, any trapping is experienced and the perfect shielding condition is still respected. Moreover, the hollow cylinder can be easily manufactured via the process of Mg liquid infiltration (Mg-RLI) [1]. A sintering technique allows also large objects to be produced (e.g. rings, cylinders, tubes, rods etc.) [18].

The literature treating the topic, either theoretically or experimentally, of cylindrical superconducting magnetic shield is vast. The efficiency of hollow cylinders in external field parallel to the cylinder axis is investigated deeply. In such an operating condition, superconducting materials show an efficiency approaching 100%, for field up to few T. But, for transversal fields, the efficiency decreases because the demagnetization factor of the cylinder changes in some extent [19, 20]. Moreover, trapped flux produces a further performance loss. These are issues of major concern to design a cylindrical shield for the aforementioned cryogenic application measurements with efficiency of 70% for this radial field configuration.

In this paper, a method for designing a MgB_2 superconducting cylindrical shield for cryogenic measurement applications by paying specific attention to the transversal field is proposed. In particular, in section II, the design process for shielding longitudinal and transversal fields is detailed. In section III, the experimental characterization of a sample cylinder is illustrated and the results are exploited to test the design procedure. Thereafter, in section IV, the case study concerning the design of a MgB_2 shield for the cryogenic DC current transformer is outlined. It is shown that the designed MgB_2 cylinder with a suitable shield sizing can allow the target requirements of 70% efficiency at 1 T in both axial and radial excitation.

2014 JINST 9 P04020

2 Design of a superconductign cylindrical annulus for shielding applications

The design of a hollow superconducting cylinder for shielding applications is aimed at identifying its geometrical dimensions for the desired efficiency at a maximum field level. Ideally, a superconducting cylinder immersed in an external magnetic field is capable of compensating the field inside its volume by generating supercurrents on its external surface. In this regards, the incident field can be decomposed in an axial and a radial component, parallel and orthogonal to the cylinder axis, respectively. These field components are counteracted by corresponding supercurrents with different paths that can be considered as superimposed separately (the reader can image two overlapped layers of surface currents). For the axial field, the cylinder can be modeled as a solenoidal coil [17–21], where the current is distributed on the surface uniformly. For the radial field, the supercurrents can be modeled as a series of symmetrical current loops distributed on opposite surfaces obtained by cutting the cylinder in half along its axis [22].

According to this model and to the tolerances on the volume to be shielded, the design can be split into two main steps:

1. Determine the dimensions inside the tolerances of volume to be shielded effectively from the axial field;

2. Adjust the dimensions in order to achieve the shield target also for the radial field.

For both the steps, the critical current density J_c of the superconducting material is to be estimated, at the required field level and for a given temperature, by corresponding models for axial and radial shield design.

2.1 Axial shielding

In a superconducting cylindrical annulus A immersed in the axial magnetic field B_{Ext} is illustrated. The annulus is modelled as a solenoidal coil of height $2h$, with an average critical current density J_c distributed uniformly along the cylinder radius r_0, and effective thickness t_{eff} for the screening currents (the equivalent internal radius of the solenoid is $r_0 - t_{\text{eff}}$). The goal of the axial shield design is to identify the height and the wall thickness $r_0 - r_i$ of the annulus, in order to guarantee the required shielding efficiency in the internal volume to be shielded (the coaxial inner cylindrical annulus Γ in grey in figure 1). The dimensions of Γ are the internal r' and external r'' radii, and the height $2h'$. For the axial shield design, the well-known results from the analysis of the field generated by a solenoidal coil are exploited [21]. The design is summarized by the following iterative procedure (figure 2):

a) Given the J_c value for the maximum external field B_{Ext} and the minimum dimensions for A (h, r_0, and r_i):

   1. Estimate t_{eff} according to the expression of the "field factor" in the central point of the cylinder by imposing $B_0 = -B_{\text{Ext}}$:

$$B_0 = J_c F(\alpha, \beta)(r_0 - t_{\text{eff}}) \tag{2.1}$$

   where F is the field factor of the solenoid, $\alpha = r_o/(r_o - t_{\text{eff}})$, and $\beta = h/(r_o - t_{\text{eff}})$ geometrical parameters; this allows to verify if the thickness of A is wide enough to

2014 JINST 9 P04020

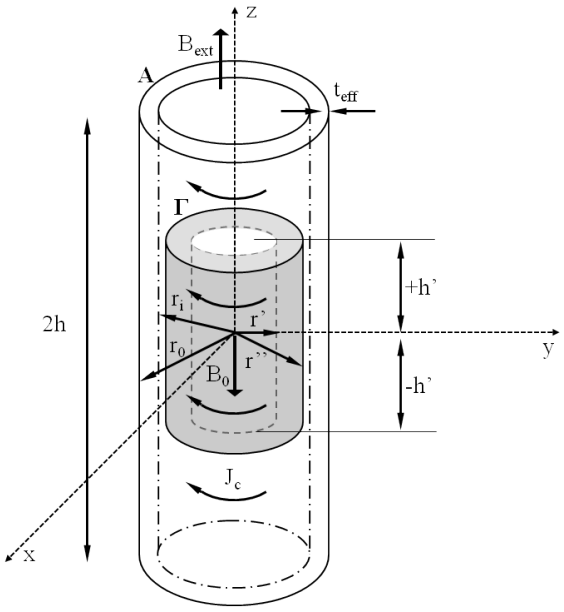

Figure 1. Solenoidal behavior of a superconducting cylindrical annulus responding to a longitudinal external field B_{Ext}.

support the screening currents for zeroing the external field at its center; conversely, the annulus dimensions have to be adjusted.

2. Assess the field in the axial positions $z = \pm h'$ in order to evaluate if the attenuation of the produced central field along the axial direction does not lead to a shielding efficiency below the target;

3. Assess the field in the radial positions r' and r'' to evaluate analogously the attenuation in the plane x, y.

The equations underlying steps 2, and 3 are [21]:

$$h_1\left(\frac{z}{r_i}\right) = 1 + E_2(\alpha,\beta)\left(\frac{z}{r_{\mathrm{int}}}\right)^2 \tag{2.2}$$

$$h_2\left(\frac{r}{r_i}\right) = 1 - \frac{1}{2}E_2(\alpha,\beta)\left(\frac{r}{r_{\mathrm{int}}}\right)^2 + \frac{3}{8}E_4(\alpha,\beta)\left(\frac{r}{r_{\mathrm{int}}}\right)^4 \tag{2.3}$$

where r is the radial coordinate, E_2 and E_4 are functions of the geometrical parameters α and β and $r_{\mathrm{int}} = (r_o - t_{\mathrm{eff}})$.

Eqs. (2.2) and (2.3) define the ratios between the axial components of the field, as a function of the height on the z-axis or the distance r from the center inside steps 2 and 3, respectively. In particular, in (2.2) and (2.3), only the first terms of an infinite series, arising from the ratio between the field expansion in spherical coordinates for a solenoid along the z- and r-axis and the field at its center, are taken into account. Higher-order terms are not considered because this approximation already provides satisfactory results.

2014 JINST 9 P04020

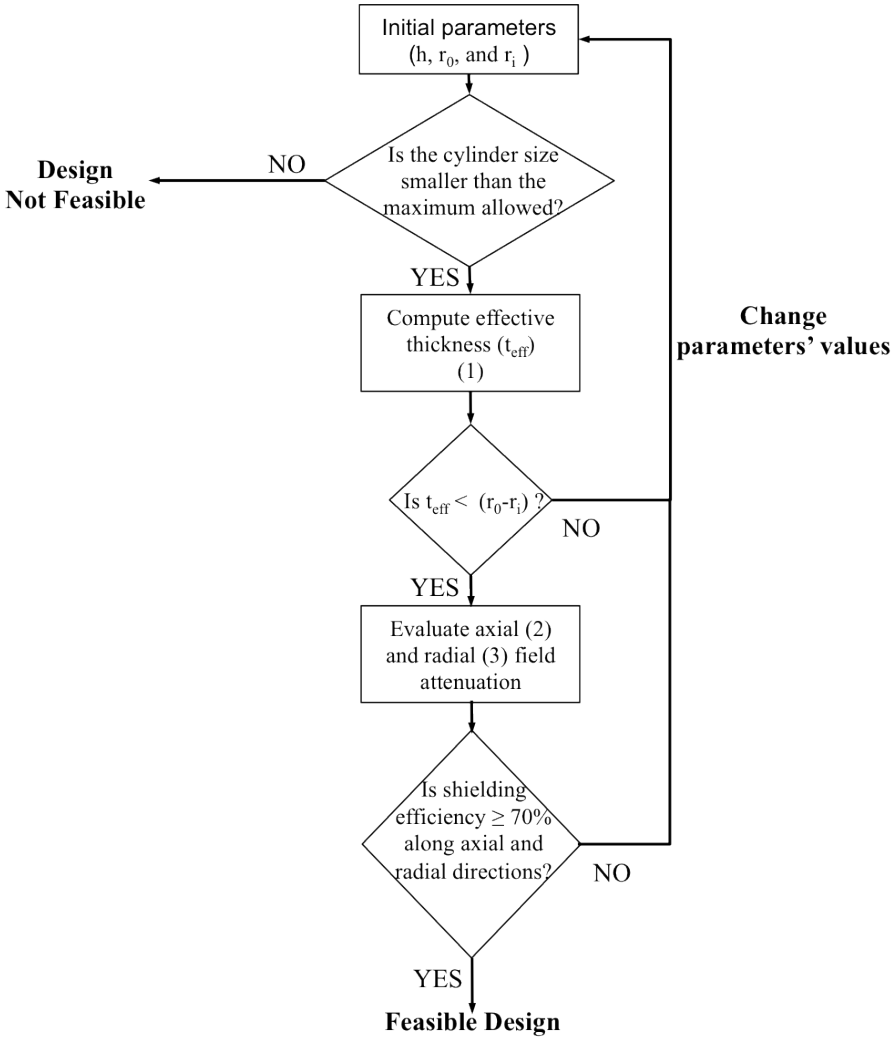

Figure 2. Procedure for axial shielding design.

b) If the results from a) lead to a shielding efficiency not lower than the target, the design is validated (figure 2); otherwise, the parameters h, r_0, and r_i are adjusted until the required efficiency is achieved. If the geometrical dimensions of cylinder exceed the maximum, the design is not feasible.

2.2 Radial shielding

For the radial design, an equivalent cylinder has to be considered by reducing the external diameter by the effective thickness of the axial shielding currents. Then, this geometry must be verified as capable of carrying the required currents. If not, the dimensions have to be adjusted by a model for the shielding currents in transversal configuration.

According to ref. [22], the response of a superconducting cylinder to transversal fields is the generation of several opposite, symmetrical current loops (figure 3). Each loop has two paths

2014 JINST 9 P04020

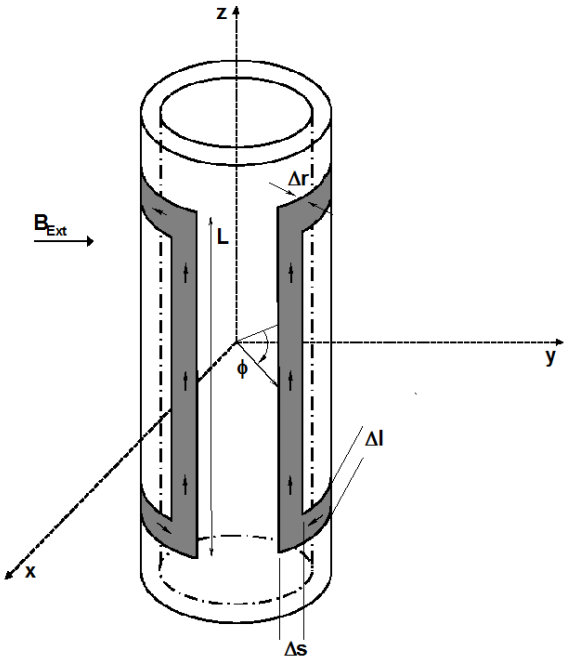

Figure 3. Typical opposite current loops (in gray) on a superconducting cylindrical annulus exposed to the radial external field B_{Ext} [22].

parallel to the cylinder axis and two coaxial paths describing an arc. The loop is characterized by the height L, the aperture angle ϕ, the widths Δs and Δl, and the thickness Δr.

For the sake of the simplicity, the design assumes two loops with ϕ equal to 45° degrees, L equal to the height of the considered cylinder, Δr equal to the half of the available thickness, and $\Delta l = \Delta s$. The field generated in the cylinder can be calculated using the Biot-Savart law [22, 23] along the external perimeter of the loops (discretizing the boundary as a superposition of straight segments). Thus, given a constant current density, the equivalent cross section surface of the currents is estimated as the ratio I/J_c, where $I = J_c \Delta r \Delta s$ is the current flowing into the loop. By assuming Δr as constant, Δs represents the loop width required to sustain the desired field. If this length is compatible with the geometry of the cylinder, the model assumption can be considered valid: a weighted series of loops overlapped on the radial direction will generate a uniform field at a constant distance from the center.

3 Experimental characterization of MgB_2 hollow cylinder in radial field

The proposed design procedure of a sample hollow cylinder exposed to radial field was validated experimentally. Moreover, measurements of shielding efficiency allow the capability of the MgB_2 material of achieving the target to be assessed.

In the following, (A) the *measurement set-up*, (B), the *experimental results*, and (C) the *discussion* of the characterization of a MgB_2 hollow cylindrical shield are illustrated.

2014 JINST 9 P04020

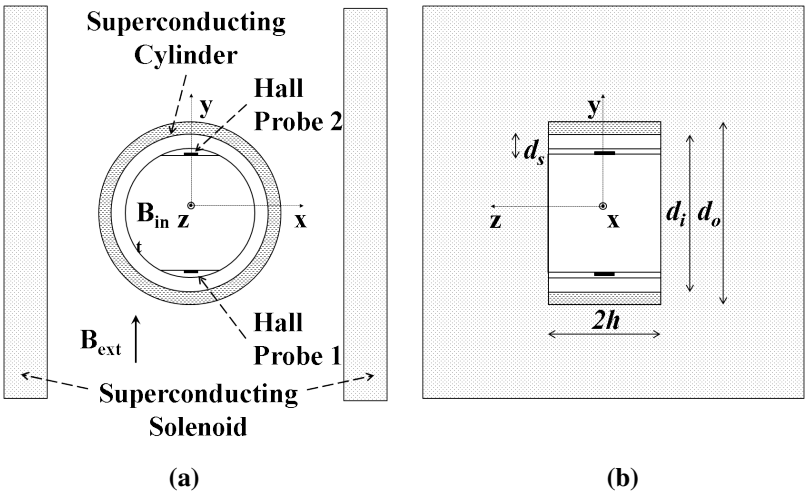

Figure 4. Schematic of the measurements set-up: cross (a) and axial (b) sections.

3.1 Measurement set-up

In figures 4, the schematic view of the measurements set-up is shown. In the superconducting cylinder (figure 4a), the axis z is disposed orthogonally to the external field B_{ext} in order to assess the radial shielding. B_{ext} is generated by a superconducting solenoid capable of providing up to 11 T. The origin of the reference (x, y, z) is placed at the center of the solenoid's field region with higher homogeneity (figure 4b). The inner and outer radii of the cylindrical annulus are labeled with d_i and d_o, respectively. Two high-sensitivity cryogenic Hall probes are mounted with the sensing area perpendicular to the y-component of the cylinder internal field B_{int}, at the half height h of the cylinder, and at distance d_s from its wall (figure 4b).

The two Hall probes were previously calibrated, without the shield, with sensitivity factors of 173.4 mVT^{-1} and 169.6 mVT^{-1}. A plastic support, with a thin ceramic strip to avoid stress at the probes' surface due to thermal contraction, is used for the superconducting material.

The sample MgB_2 hollow cylinder has the height $2h$ of 40 mm, the inner diameter d_i of 56 mm, and the thickness $(d_o - d_i)/2$ of 4.5 mm. The length d_s is about 6 mm. In figure 5a, the sample preparation for the cylinder of MgB_2 is shown before its installation in the cryogenic insert. Once the sample is connected to the cryogenic insert, the shaft is introduced in the warm cryostat where the magnet bore is housed (figure 5b). The cool down by liquid helium is started to reach 4.2 K in zero field condition.

3.2 Measurement results

Two sets of tests were carried out with the Hall probes placed (i) in reference position (such as pointed in figure 4a), and (ii) rotated by 90° counterclockwise.

3.2.1 Reference position

In this test, the external field was ramped up and down from 0.0 to 1.2 T, but by cycling at 0.7 and 1.0 T. In the initial part of the test, the external field B_{Ext} is ramped from 0.0 T to 0.6 T at 0.6 Tmin^{-1}. In figure 6a, the radial field B_{Int} measured by the Hall probes inside the MgB_2

2014 JINST 9 P04020

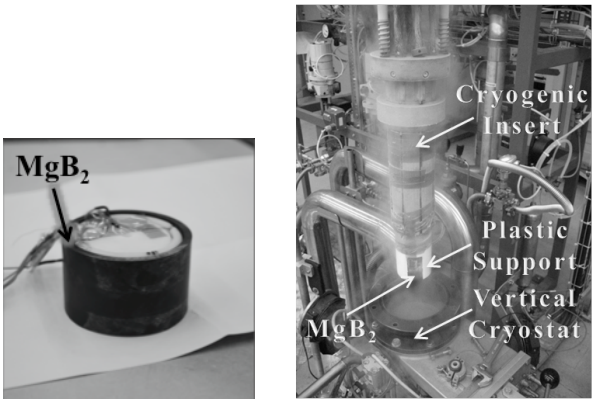

(a) (b)

Figure 5. Sample cylinder of MgB_2 before installation (a), and into the measurement set-up (b).

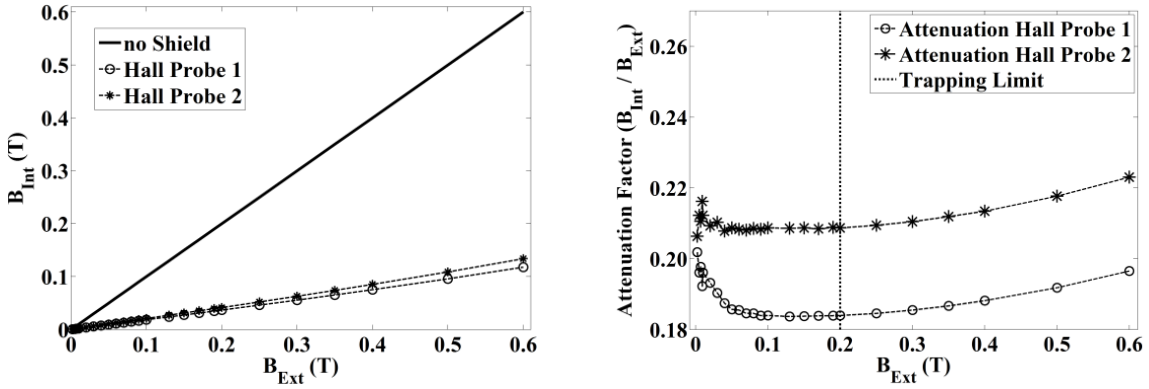

(a) (b)

Figure 6. Measured radial field (a) and attenuation ratio (b) for the Hall probes 1 (o) and 2 (*) inside the MgB_2 cylinder: (-) without shield (a) and (—) trapping limit (b).

cylinder is illustrated. The probes signals acquired at several plateaus of B_{Ext} do not exhibit significant time dependence. The full line represents the field without shielding. The difference in the field measured by the 2 probes (o,*) could depend on a residual tilt angle. Figure 6b shows the attenuation (or shielding) factor of the cylinder, i.e the ratio betweenB_{Int} and B_{Ext}. An efficiency of about 80% is achieved. The vertical dashed line highlights the boundary of the region without flux trapping: the shielding factor is almost constant. This is highlighted in figure 7, where a base line, calculated as linear fit of the data up to 0.6 T, is subtracted to the measured data of the probes.

In figures 8, the overall measurement set of the test as a whole from 0.0 to 1.2 T is displayed, by distinguishing results of probe 1 (a) and 2 (b). In particular, the arrows mark increasing and decreasing B_{Ext}. In the above-described first part of the test from point 1 to 2, the field is increased up to 0.7 T. From point 2 to 3, a trapping of almost 10 mT is highlighted by the straight-line, owing to the field ramp down to 0.1 T and up back to 0.7 T. Along points 4 and 5, the field is again increased up to 1.2 T. At $B_{\mathrm{Ext}} = 1.0$ T, the signals of the Hall probes are still time-independent

2014 JINST 9 P04020

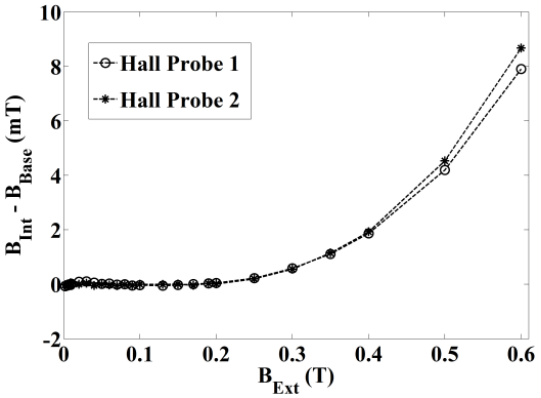

Figure 7. Measured trapped flux in the MgB_2 cylinder for external field up to 0.6 T, obtained by subtracting the base line identified using the data up to 0.2 T.

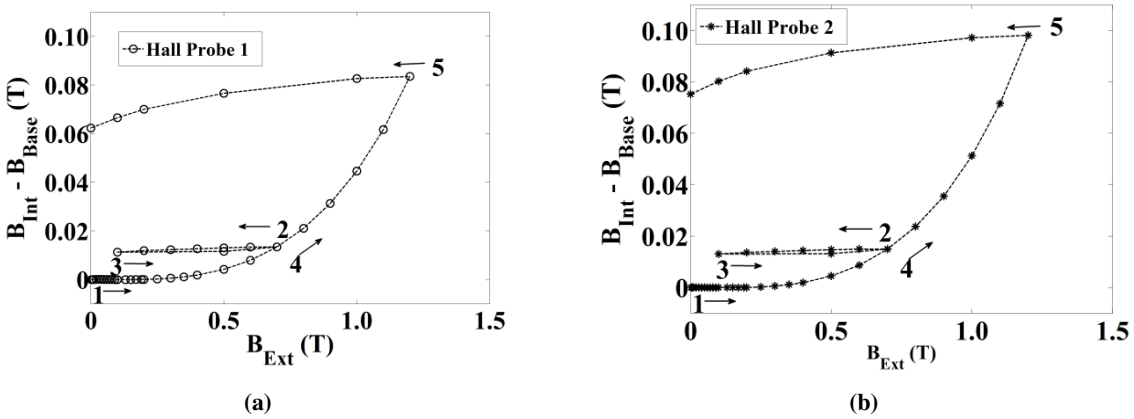

Figure 8. Measured trapped flux in the MgB_2 cylinder for external field sweep up to 1.2 T: probe 1 (a) and 2 (b); the arrows highlight the ramp direction of the external field.

without any penetration phenomena. From the initial 80%, the shielding efficiency, owing to the trapped field, decreases to 74% and 72% for probe 1 and 2, respectively. Afterwards, the field is decreased down to 0.0 T. From external fields above 1.2 T, penetration phenomenon starts and the stability of the shield is lost.

3.2.2 Rotaded position

A further investigation was carried out in order to verify the shielding unformity in the cylinder. At this aim, the Hall probes were rotated by 90°, counterclockwise with respect to the reference position of figure 4, in order to measure the x component of the internal field, ideally null. As for tests in reference position, the external field was ramped up and down from 0.0 to 1.2 T, but in this case by twofold cycling at 0.7 and 1.0 T.

Also in this case, in the initial part of the test, the external field B_{Ext} is ramped from 0.0 to 0.6 T at 0.6 Tmin^{-1}. In figures 9, the x-component of the internal field (a) and the attenuation factors (b) measured by the two Hall probes (1: o, and 2: *) are illustrated. The attenuation factor

2014 JINST 9 P04020

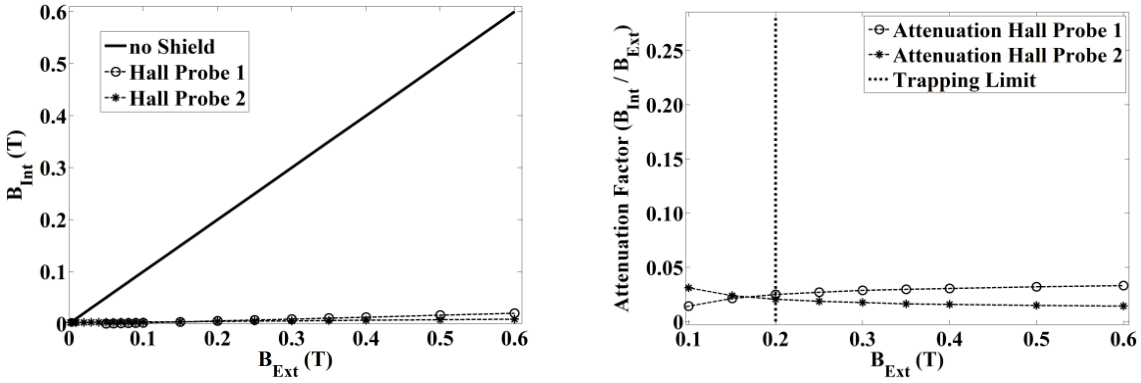

Figure 9. Measured x-component of the internal field (a) and attenuation ratio (right) for the Hall probes 1 (o) and 2 (*) rotated of 90° degrees: (-) no shield (left) and (—) trapping limit (b).

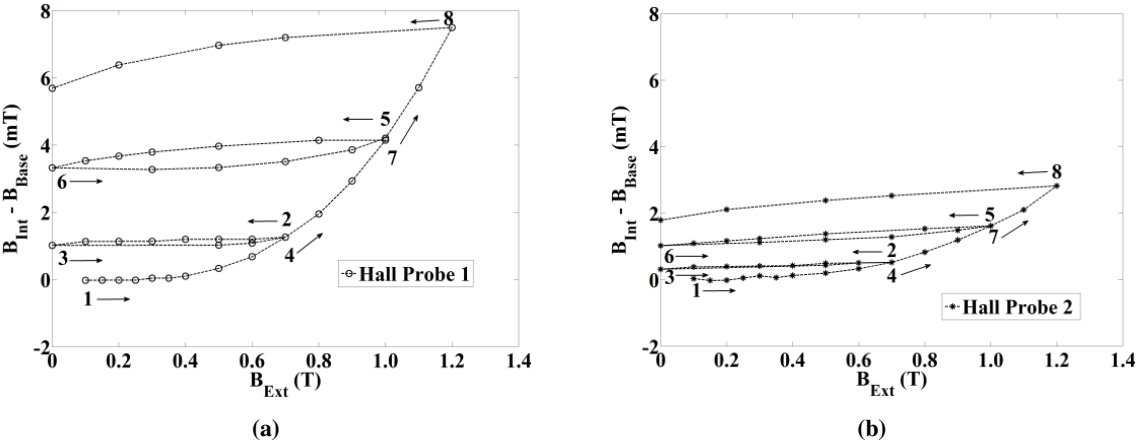

Figure 10. Measured x-component of trapped flux in the MgB_2 cylinder for external field sweep up to up to 1.2 T: probe 1 (a, o) and 2 (b, *); the arrows highlight the ramp direction of the external field.

is of the order of 0.02 ($B_{\mathrm{Ext}} \leq 0.2$ T), giving rise to a field uniformity of 98%. The differences in the probes readings could be due to a tilt with respect to the ideal 90° degrees reference, meaning that a smaller uniformity improvement is expected by a better alignment.

In figures 10, the trapped flux is assessed in the direction x, by distinguishing probe 1 (a) and 2 (b) is shown. As expected, by cycling at 0.7 T (points 2, 3, and 4) and 1.0 T (points 5, 6, and 7), the trapped flux is almost constant. Therefore, the shield performance can be roughly modelled by the base line shifted by the trapped field at the considered external field value. This is true as far as penetration starts. The field uniformity at 1.0 T is 97% for a maximum-trapped field of 24 mT.

3.2.3 Discussion

The tests on the MgB_2 sample have shown the capability of this superconducting material to support screening currents with a shielding efficiency for radial excitation better than 70% up to 1 T. The

2014 JINST 9 P04020

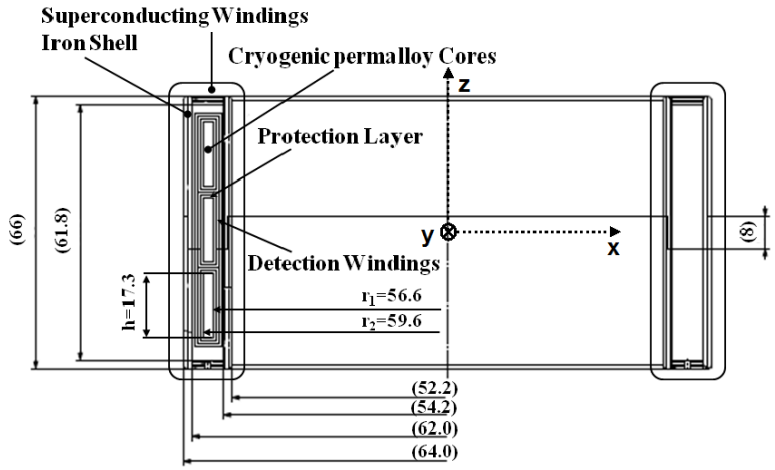

Figure 11. Cross-section view of the DCCT sensing element proposed in ref. [10] (lengths in mm); on the left: detail of the structure.

uniformity of the shielding effect was assessed by measuring the orthogonal component of the field inside the cylinder. A maximum value of 24 mT is recorded for such a component; this gives rise to uniformity of 97% with respect external field. By assessing the current distributions on the cylinder surface, the design of a shield with desired dimensions and performance can be carried out.

4 Case study: cryogenic DC current transformer

In figure 11, the cross section of a sensing element [10] for a cryogenic DCCT designed for measuring currents up to 100 kA is depicted. On the left part, a detail of the coaxial structure is given. In particular, the cores of a soft Ni 81-Mo 5-Fe magnetic alloy (cryogenic permalloy) allow limitations of μ-metal magnetic characteristics at cryogenic conditions to be overcome. The inner and the outer radii of the cores are chosen in order to maximize the distance from the cable and to have enough space in the radial direction x for other elements. Each core is endowed with a thin protection layer (1 mm) of Epoxy to bear mechanical stresses during winding. The detection coil is wound with 200 turns of an insulated copper wire with a diameter of 0.315 mm. The compensation coil is wound with 8,000 turns of type 1 LHC corrector strand [24] (estimated thickness of 5.22 mm), outer diameter 0.435 mm. The strand has a critical current of 76.2 A at 4.2 K and for an external field of 4 T. An iron shell between the cores and the compensation winding avoids off-centring of the cable under test that could lead to a performance loss of the DCCT, and, even to core saturation.

In the design [10], a superconducting magnetic cylinder (owing to the favorable temperature of operation), combined with the pure iron thin shell (2 mm thick), is needed for shielding the cores from external fields. Total efficiency results from the iron's action (up to 0.3 T), combined with the effect of the generated superconducting currents for the full range from 0 to 1 T. Thus, the superconducting cylinder has to guarantee an attenuation of 70% for external fields of 1 T inside the iron shell.

2014 JINST 9 P04020

The sensing element can be housed in a cylinder with minimal dimensions of 140 mm inner diameter along the radial direction x and 76.4 mm of height on the axial direction z. A maximum wall thickness of 6 mm is allowed from the overall imposed size. The homogeneous region of shielding is represented in the structure detail of figure 11 by the section of the iron shield. Therefore, along z, the target efficiency has to be guaranteed over 66 mm, and, along x, over 11.8 mm (i.e., the width of the iron shell, 64.0–52.2 mm), where the cores are housed actually. These values are the requirements for the design of a MgB_2 cylindrical superconducting shield. According to the design procedure of section II, the design is carried out separately for the axial and radial field.

4.1 Axial design

According to ref. [17], for a maximum axial field of 1 T to be shielded, an average critical current density J_c of 100 kAcm^{-2} with constant distribution along the cylinder radius can be assumed. Following the procedure of figure 2, the effective thickness t_{eff} of the screening currents is estimated by eq. (2.1). The required thickness is 1.2 mm to generate 1 T, at the centre of the cylindrical shield of minimal dimensions. Then, it can be stated that the MgB_2 bulk cylinder of required dimension is capable of shielding effectively 1 T at its centre. However, the design target is to verify that an efficiency of 70% is guaranteed in the iron shell region: $z = \pm h'$, $h' = 33$ mm, $r' = 52.2$ mm, and $r'' = 64$ mm (figure 1). By considering the cylinder height of 76.4 mm and a central shielding field of 1 T, the ratio in eq. (2.2) at $z = 33$ is $h_1 = 0.72$. This means a shielding field of 0.72 T at that position. Then, a residual field of 0.28 T can be assumed, and an efficiency of 72% is achieved. By evaluating eq. (2.3) at r'=52.2 mm and r"=64.0 mm, results are worse, $h_2 = 1.34$ (52.2 mm) and $h_2 = 1.52$ (64.0 mm): the efficiency, considering the module of the field, is decreased down to almost 50%. The solution for this problem is to increase the height of the cylinder. The maximum height easily realizable by the RLI technology for this MgB_2 cylinder is 120 mm. In this case, the efficiency along the z-axis is of the order of 90%, and for the x-direction of the order of 80% in the iron shell region: the required efficiency is then largely achieved.

4.2 Radial design

According to axial design, the cylindrical shell of MgB_2 has the following dimensions:

- Internal diameter: 140 mm;
- External diameter: 152 mm;
- Height: 120 mm.

Furthermore, the actual computed thickness of the axial shielding currents is 0.94 mm; therefore, the effective external diameter for shielding radial fields is 150.12 mm. According to these constrains, the capability of this equivalent cylinder of supporting the required current in order to achieve transversal efficiency of 70% is to be verified.

According to the procedure of section II.B, the experimental data from the MgB_2 sample characterization measurements (section III) are analyzed for design purposes. At 1 T, the shielding efficiency of the tested cylinder is 74% at the position of the Hall probe 1, and the shielding field is then 0.74 T. From the Biot-Savart calculation, a total current of 20.39 kA is required on the

cylinder's bulk. The circular and the lateral paths of the loop are discretized in 200 and 2 segments, respectively. If the current density J_c is assumed to be 100 kAcm^{-2}, as for the axial design, the equivalent cross section area of 0.2 cm^{-2} is estimated for the loop currents. This leads to $\Delta s =$ 0.9 cm, perfectly admissible in the shield geometry.

Following the same steps of the analysis of the measurement data and using the dimensions of the MgB_2 shield, the current loop required to produce 0.74 T at 64 mm far from the cylinder axes is 47.1 kA. This means an equivalent cross section area of 0.47 cm^{-2}. The equivalent width of the current loops is $\Delta s = 1.8$ cm, still perfectly admissible in the shield geometry. According to that, the same calculation can be carried out at 52.2 mm. In this position, the estimated field value, using 47.1 kA, gives rise to efficiency of the order of 60%. This is not of concern, because the internal part of the iron shell is already screened by the external one. Moreover, due to the simplicity of the model assumption, the dependency on the y-direction has to be thought as a worst case. In other words, the MgB_2 cylindrical shield with the required dimensions will provide the target efficiency of 70% in the radial direction at the middle plane of the cylinder in the region of interest. This performance holds in the z-direction along the height of the iron shell.

5 Conclusions

The design of a MgB_2 cylindrical superconducting shield for cryogenic measurement applications in background field of 1 T is proposed. The design is based on the exploitation of MgB_2 material manufactured by the reactive Mg liquid infiltration process, an 'in-situ' technology able to give very-dense MgB_2 objects. Characterization measurements of a MgB_2 sample cylinder provides the required bases for the feasibility study of the shield. In particular, it was experimentally proven on the sample a 74% shielding efficiency for a background transversal field of 1.0 T at 4.2 K.

The geometrical design is carried out both for axial and radial field configurations. The optimization of the cylindrical shields dimensions is based also on the exploitation of measurements data from the experimental characterization of MgB_2 samples cylinders at 4.2 K. In particular, the results reported in this paper are exploited in the radial project, by using conversely for the axial design previous results [17].

The design is carried out by modeling the shielding currents on the cylinder inside by well-established techniques. The experimental results provide the mean to validate the model. The numerical results show the overall performance of the designed cylinder matches with the target of 70% efficiency in both the background field configurations.

The designed MgB_2 cylinder is already in the production phase and further work will be aimed at exploiting it as effective shield for a cryogenic DCCT prototype.

Acknowledgments

This work is supported by CERN through the agreement K1776/TE with the University of Sannio, whose support authors acknowledge thankfully. The authors gratefully thank L. Bottura, F. Cennamo and A. Figini Albisetti for their contribution, useful suggestions, and cooperation, as well as the Building 163 team for the support during the experiments.

2014 JINST 9 P04020

References

[1] G. Giunchi, *High density MgB_2 obtained by reactive liquid Mg infiltration*, *Int. J. Mod. Phys.* **B 17** (2003) 453.

[2] R. Minet, H. A. Combet, J. Y. Le Traon and J. Schmouker, *Contribution to the Use of Superconducting Shield fo Magnetic Field Shaping*, *IEEE T. Mag.* **3** (1967) 271.

[3] K. Sinokita, R. Toda and Y. Sasaki, *Construction of Compact MRI Magnet with Superconducting Shield*, *J. Phys. Conf. Ser.* **150** (2009) 012041.

[4] Z.Y. Zhang, S. Matsumoto, S. Choi, R. Teranishi and T. Kiyoshi, *Comparison of Different Configuration of NbTi magnetic Lenses*, *Supercond. Sci. Technol.* **24** (2011) 105012.

[5] K. Grohmann, H.D. Hahlbohm, H. Lubbig and H. Ramin, *Ironless Cryogenic Current Comparator for AC and DC applications*, *IEEE T. Instrum. Meas.* **23** (1974) 261.

[6] K. Knaack et al., *Cryogenic Current Comparator for Absolute Measurements of The Dark Current of Superconducting Cavities for Tesla*, in proceedings of 8^{th} *European Particle Accelerator Conference*, Paris, France (2002), p. 1915.

[7] W. Meng, W.B. Sampson and M. Suenaga, *Magnetic Flux Shield for the Precision Moun g-2 Storage Ring Superconducting Inflector*, *IEEE T. Mag.* **30** (1994) 1766.

[8] S.J. St. Lorant, *Superconducting Shield for Magnetic Flux Exclusion and Field Shaping*, in proceedings of *International Conference on Magnet Technology*, Upton, N.Y., U.S.A. (1972), p. 227.

[9] K. Kamiya, B.A. Warner and M.J. DiPirro, *Magnetic Shield for Sensitive Detector*, *Cryog.* **41** (2001) 401.

[10] P. Arpaia, A. Ballarino, L. Bottura and G. Montenero, *Cryogenic sensing element for measurement current transformers*, 2014 *JINST* **9** P03011.

[11] C. Berriaud and A. Donati, *A device for measuring high current at cryogenic temperatures*, *IEEE T. Appl. Supercond.* **12** (2002) 1264.

[12] T. Rikitake, *Magnetic and Electromagnetic Shielding*, Terra Scientific Publishing Company, Tokio, Japan (1987).

[13] H.W. Veirjers, A. Godeke, B. Ten Haken, S. Wessel and H.H.J. Ten Kate, *Improved Superconducting Direct Current Feter for 25–50 kA*, *Adv. Cryog. Eng.* **39** (1994) 1147.

[14] I. Itoh, T.Sasaki and H. Otsuka, *NbTi/Nb/Cu Multilayer Composite Materials for Superconducting Magnetic Shielding –Superconducting Performance and Microstructure of NbTi Layers*, Nippon Steel Technical Report **85** (2002) 118.

[15] I. Itoh, T.Sasaki, S . Minamino and T.Shimizu, *Magnetic Shielding Properties of NbTi/Nb/Cu Multilayer Composite Tubes*, *IEEE T. Appl. Sup.* **3** (1993) 177.

[16] T. Sasaki, K. Iwata, H. Otsuka and I. Itoh, *Generation of homogeneous high magnetic fields within superconducting 'Swiss roll'*, *Cryog.* **35** (1995) 339.

[17] J.J. Rabbers, M.P. Oomen, E. Bassani, G. Ripamonti and G. Giunchi, *Magnetic shielding capability of MgB_2 cylinders*, *Supercond. Sci. Technol.* **23** (2010) 125003.

[18] G.Giunchi, G.Ripamonti, T.Cavallin and E.Bassani, *The reactive liquid Mg infiltration process to produce large superconducting bulk MgB_2 manufacts*, *Cryog.* **46** (2006) 237.

[19] J.-F. Fagnard, M. Dirickx, M. Ausloos, G. Lousberg, B. Vanderheyden and Ph. Vanderbemden, *Magnetic shielding properties of high-Tc superconducting hollow cylinders: model combining experimental data for axial and transverse magnetic field configurations*, *Supercond. Sci. Technol.* **22** (2009) 105002.

2014 JINST 9 P04020

[20] A. Sanchez and C. Navau, *Magnetic Properties of Finite Superconducting Cylinders. I. Uniform Applied Field*, *Phys. Rev.* **B 64** (2001) 214506.

[21] Y. Iwasa, *Case Studies in Superconducting Magnets*, Springer Science, New York, U.S.A. (2009).

[22] D.J. Frankel, *Model for Flux Trapping and Shielding by Tubular Superconducting Samples in Transverse Fields*, *IEEE T. Mag.* **5** (1979) 1349.

[23] M. Wilson, *Superconducting Magnets*, Oxford University Press, Oxford, U.K. (1987).

[24] C.H. Denarieì, A. Hilaire and R. Wolf, *Critical Current Measurements of LHC Superconducting Corrector Magnet Strands*, AT-MEL Technical Note, Edms no. 564604, 31 January 2005.

2014 JINST 9 P04020